Chinese Chemical Letters 35 (2024) 108600

Contents lists available at ScienceDirect

Chinese Chemical Letters

journal homepage: www.elsevier.com/locate/cclet

Efficient blue-light-excitable copper(I) coordination network phosphors for high-performance white LEDs

Pingping Wang[1], Huixian Miao[1], Kechuan Sheng, Bin Wang, Fan Feng, Xuankun Cai, Wei Huang*, Dayu Wu*

Jiangsu Key Laboratory of Advanced Catalytic Materials and Technology, Advanced Catalysis & Green Manufacturing Collaborative Innovation Center, School of Petrochemical Engineering, Changzhou University, Changzhou 213164, China

ARTICLE INFO

Article history:
Received 9 April 2023
Revised 15 May 2023
Accepted 22 May 2023
Available online 24 May 2023

Keywords:
Metal-organic framework
Coordination polymer
Photoluminescence
Phosphor material
White-light LED
Phosphor-converted LED

ABSTRACT

The blue-light-excitable phosphors play a crucial role in the high-performance white LEDs. Here, we report on two new Cu(I) coordination network materials as yellow-emitting phosphors prepared by suitably expanded π-conjugated triazole ligands. Upon blue-light irradiation, these complexes exhibit efficient solid-state emission and enhanced photostability. Through incorporating the yellow phosphor and a commercial blue-green powder ($BaSi_2N_2O_2:Eu^{2+}$) with a blue LED chip, the phosphor-converted LED devices display remarkable white emission properties. The experimental results demonstrate that the Cu(I) coordination network materials function as promising blue-light excitable phosphors with great application potential for full-spectrum white LEDs.

© 2024 Published by Elsevier B.V. on behalf of Chinese Chemical Society and Institute of Materia Medica, Chinese Academy of Medical Sciences.

Light-emitting diodes (LEDs) are highly attractive candidates for next-generation lighting and display applications because of their many advantages, such as high effciency, long operation lifetime, and good reliability [1–6]. White LEDs (wLEDs) with high color rendering index (CRI) and ideal correlated color temperature (CCT) for indoor lighting can be conventionally obtained through exciting the yellow phosphors with a blue-emitting LED chip [7–13]. For example, the integration of a blue InGaN LED chip (420–480 nm) with yellow phosphor, $Y_3Al_5O_{12}:Ce^{3+}$ (YAG:Ce^{3+}), is generally used to fabricate commercial wLEDs [14–16]. In consideration of sustainable development and environmentally friendly LED technologies, the development of inexpensive metal complexes as efficient yellow phosphors for substituting rare-earth-based wLEDs is highly demanding [17–20]. Recently, metal halide complexes have been widely investigated as a kind of promising phosphor, because they show a wide excitation band in the UV region, tunable emission band and intense brightness [21–25]. Among them, the Cu halide cubic clusters with the formula of $[Cu_4\times_4L_4]$ (X = Cl, Br, I; L = N- or P-terminal ligands) exhibit the outstanding photoluminescence (PL) with high quantum yield [26–35]. However, a major shortcoming of this type of complex is their low photochemical stability under the condition of ultraviolet irradiation [36–38]. In addition, this kind of complex typically suffers from the poor absorption band in the visible region, which is not appropriate for blue-emitting GaN LED chips. Hence, the development of high-performance Cu(I)-based white LEDs with broadband excitation band and superior thermal stability that can meet the requirements of commercial applications still remains a challenge.

In this work, we report on the synthesis, structure and photophysical properties of Cu(I) coordination polymers with suitably expanded π-conjugated triazole ligands so that the excitation wavelength covers a wide spectral band from UV to blue region. The triazole derivative ligands, [1,2-bis((1*H*-benzo[*d*][1,2,3]triazol-1-yl)-methyl)benzene (bbtmb) and 1,2-bis((5-methyl-1*H*-benzo[*d*][1,2,3]triazol-1-yl)methyl)benzene (bmtmb), have been synthesized for preparation of their copper coordination network phosphors, $[(bbtmb)Cu(CN)]_n$ (**CP1**) and $[(bmtmb)_2Cu_4I_4]_n$ (**CP2**). The broad excitation bands in the blue region have been observed for the as-synthesized coordination network phosphors. The phosphor-converted white LEDs (pc-wLED) were fabricated by incorporation of the copper(I) coordination polymers as phosphor with a 428 nm emitting InGaN chip. Impressively, under blue light excitation, the optimal **CP1**-prototype pc-wLED showed outstanding white emissions with ideal CIE color coordinate and high color rendering index.

The coordination networks, **CP1** and **CP2** were synthesized from benzotriazole-based ligands and metal salts under solvothermal condition. The powder XRD patterns match well with the calcu-

* Corresponding authors.
E-mail addresses: whuang@cczu.edu.cn (W. Huang), wudy@cczu.edu.cn (D. Wu).
[1] These authors contributed equally to this work.

https://doi.org/10.1016/j.cclet.2023.108600
1001-8417/© 2024 Published by Elsevier B.V. on behalf of Chinese Chemical Society and Institute of Materia Medica, Chinese Academy of Medical Sciences.

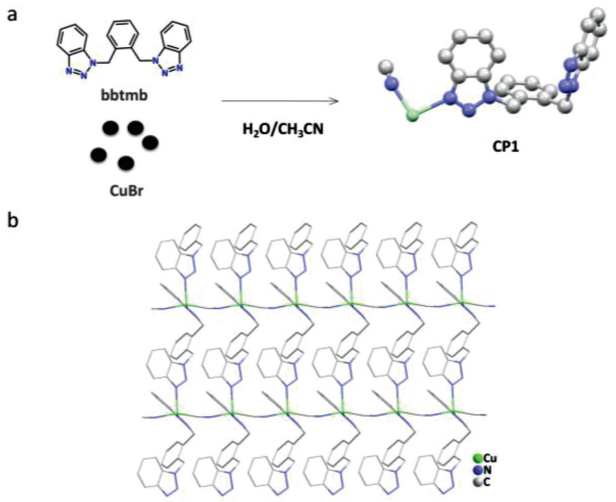

Fig. 1. (a) The synthesis and X-ray crystal structure of **CP1**. (b) Two-dimensional network structure of **CP1**. Color code: Cu, green; N, blue; C, gray. All hydrogen atoms are not shown for clarity.

lated ones from single-crystal X-ray diffraction (SC-XRD) data, indicating the phase purity of the bulk crystals (Fig. S1 in Supporting information). The analysis of SC-XRD at 100 K revealed that **CP1** (CCDC: 2262906) and **CP2** (CCDC: 2262907) crystallized in the triclinic *P*1 and in the monoclinic *C*2/*c* space group, respectively (Table S1 in Supporting information). The asymmetric unit of **CP1** consists of one crystallographically unique Cu(I), a ligand bbtmb, as well as a cyanide anion (Fig. 1a). The presence of cyanide anion in the structure was further confirmed by the IR absorption band at 2102 cm^{-1}, assignable to a strong $\nu_{C\equiv N}$ stretching band (Fig. S2 in Supporting information). The cyanide species may originate from the decomposition of acetronitrile solvent molecule under solvothermal condition. The four-coordinate Cu centers possess a distorted octahedral {CuN_3C} coordination environment, which is held by two N atoms from two different ligands, bbtmb (Cu1–N6 = 2.181(5) Å and Cu1–N8=2.052(7) Å), one N atom from the cyanide (Cu1–N1 = 2.257(5) Å), and one C atom (Cu1–C21 = 1.960(7) Å) from another cyanide (Table S2 in Supporting information). As shown in Fig. 1b, the **CP1** features a 2D coordination polymer assembled from Cu(I) nodes and μ-L cyanide anions and μ-bbtmb linkers. Both the μ-CN and μ-bbtmb act as terminal linkers, and interconnect the adjacent copper centers along the crystallographically different directions into a 2D metal−organic layer.

The asymmetric unit of **CP2** consists of two interconnected Cu(I) ions and two I anions plus one organic linker ligand, bmtmb (Fig. 2a). The crystal structure of tetranuclear copper(I)−iodide cluster in **CP2** exhibits a heavily distorted staircase structure as shown in Fig. 2b. In the tetranuclear [Cu_4I_4] cluster, there are two types of Cu(I) centers with slight different tetrahedral geometries. Cu1 is four-coordinated with one μ_3- and one μ_2-I, and two benzotriazole N donors from the different ligands with the distorted tetrahedral sphere (Table S3 in Supporting information). However, Cu2 is four-coordinated with one μ_2- and two μ_3-I and one N-donor from a benzotriazole. All Cu(I) atoms are interlinked by bridging μ_2- or μ_3-I atoms to form the rhomboidal Cu−I_2−Cu units with Cu···Cu distances in the range of 2.629(2)−2.759(2) Å at 100 K. The shortest intermetallic distance is much shorter than the sum of the van der Waals radii of the copper atoms (2.8 Å), indicating significant cuprophilic interaction (d^{10}–d^{10}) in the structure [39–44]. In the structure of **CP2**, the staircase Cu_4I_4 clusters are interlinked *via* two neighbor Cu–N bonds by a pair of bmtmb ligands, giving rise to a 1D cluster-based coordination network (Fig. 2c). The centroid···centroid distance between two phenyl rings from a pair of benzotriazole linker ligands is found to be 4.152 Å, which is suggestive of the weak $\pi\cdots\pi$ stacking interaction (Fig. S3 in Supporting information) [45].

At room temperature, both **CP1** and **CP2** exhibit the wide excitation band covering from deep-UV to blue-light region (Fig. 3a). **CP1** and **CP2** exhibit a strong emission band centered at 596 and 560 nm, respectively, with the full width at half maximum (FWHM) of about 140 nm. The PL quantum yields (PLQYs) in the solid state are determined to be 44.46% and 27.04% for **CP1** and **CP2** (Table 1 and Fig. S4 in Supporting information). In the excitation-dependent PL emission spectra, **CP1** exhibits the strongest PL emission under the excitation wavelength at 400 nm, while **CP2** exhibits the strongest emission at 450 nm (Figs. 3b and c). In order to investigate the emission origin, the PL decay experiments and the excited-state (ES) decay analysis were performed (Figs. S5 and S6

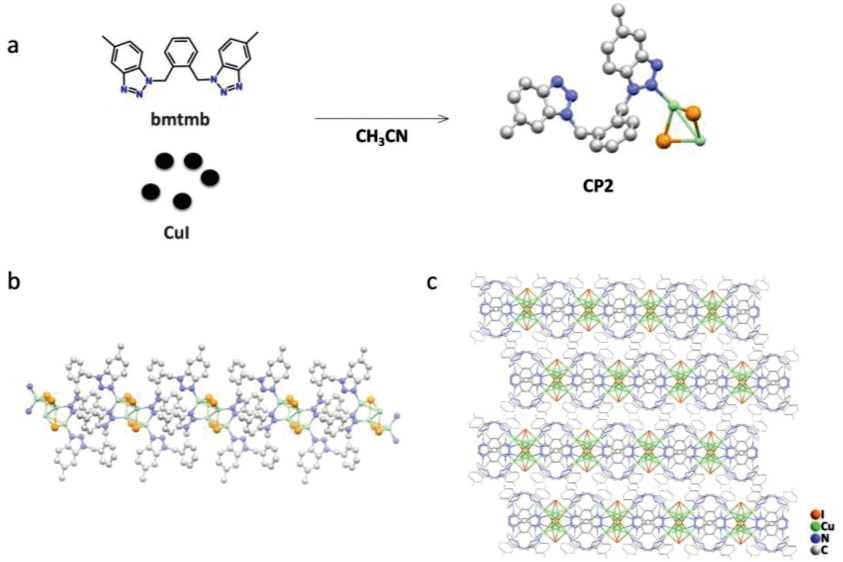

Fig. 2. (a) The synthesis and X-ray crystal structure of **CP2**. (b) The 1-D chain structure of **CP2**. (c) The 2-D structure of **CP2**. Color code: Cu, green; I, orange; N, blue; C, gray. All hydrogen atoms are not shown for clarity.

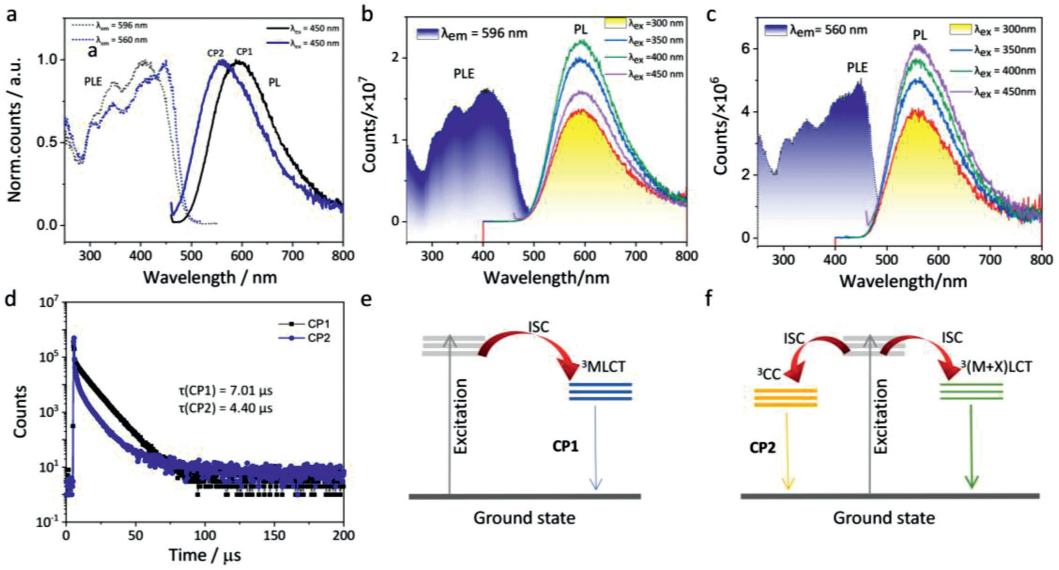

Fig. 3. (a) PL excitation and emission spectra of **CP1** and **CP2** samples at 298 K. (b) PL spectra of **CP1** under various excitation wavelengths. (c) PL spectra of **CP2** under various excitation wavelengths. (d) Excited-state decay profiles of **CP1** and **CP2** at room temperature. (e) Excited-state decay pathways of CP1. ^{3}MLCT, metal-ligand charger transfer transition. (f) Excited-state decay pathways of CP2. ^{3}(M + X)LCT, mixed metal– & halide–ligand charger transfer transition; ^{3}CC, cluster-centered transition; ISC, intersystem crossing; Superscript '3' refers to triplet excited state.

Table 1
Photophysical data of **CP1** and **CP2** in the crystalline state.

Comp.	PLE peak (nm)	PL peak (nm)	FWHM (nm)	PLQY (Φ_{PL},%)	τ (μs)	k_r[a] (10^4 s^{-1})	k_{nr}[b] (10^4 s^{-1})
CP1	400	596	140	44.46	7.01	7.10	8.87
CP2	450	560	140	27.04	4.40[c]	5.51	14.86

[a] Radiative rate constant calculated $k_r = \Phi_{PL}\tau$.
[b] Nonradiative rate constant calculated $k_{nr} = (1 - \Phi_{PL})/\tau$.
[c] The average τ is calculated according to the formula, $\tau_{av} = (B_1\tau_1^2 + B_2\tau_2^2)/(B_1\tau_1 + B_2\tau_2)$.

in Supporting information). The PL lifetime (τ) for **CP1** is determined to be 7.01 μs based on the monoexponential decay function, typical of ^{3}MLCT emission origin (Figs. 3d and e). However, the ES decay curve of **CP2** obeys the biexponential decay function with the $\tau_1 = 1.12$ μs and $\tau_2 = 5.72$ μs (Table S4 in Supporting information), and the average $\tau_{av} = 4.40$ μs, which is indicative of different phosphorescence mechanism between **CP2** and **CP1** [46]. The dual lifetime components indicate an additional radiative relaxation pathway is operative for **CP2** in addition to ^{3}(M + X)LCT, which may arise from the cluster-centered (^{3}CC) band common in the presence of cuprophilic interactions (Fig. 3f).

The radiative decay rate (k_r) is estimated through the equation $k_r = \Phi_{PL}\tau^{-1}$ to be 7.10×10^4 s^{-1} and 5.51×10^4 s^{-1} for **CP1** and **CP2**, respectively (Table 1). Considering $\Phi_{PL} = k_r/(k_r + k_{nr})$, where k_{nr} represents the rate of the nonradiative process, the value of k_{nr} is estimated to be 8.87×10^4 s^{-1} and 14.86×10^4 s^{-1} for **CP1** and **CP2**, respectively. Hence, the increase of the quantum yield of **CP1** is related to the combined effects, such as increase of radiative rate by a factor of 1.3 and a decrease of the nonradiative rate by a factor of 1.6 as compared to **CP2**. In the presence of strong binding of cyanide with Cu(I), the small proportional involvement of −CN groups in molecular vibrations favors less structure distortion, and the reorganization energy can be suppressed significantly, thereby giving rise to the reduced k_{nr} value to a large degree and increasing quantum efficiency. Hence, the rigid structure of cyanide-bridge framework in **CP1** is one of the main causes for the reduction of nonradiative process. The large k_{nr} value in **CP2** is caused by the strong vibration of its substituent methyl groups, resulting in severe structural distortion in the process of electron transition and thereby reducing quantum efficiency [47].

To investigate thermal stability of the PL emission, the temperature dependence of PL was investigated in the wide temperature range, which shows the slightly different temperature-dependent emission shift for **CP1** and **CP2**. As the temperature gradually increases from 80 K to 500 K, the emission center of **CP1** exhibits a small blue shift by about 12 nm. In contrast, the emission center of **CP2** shows a small bathochromic shift (*ca.* 7 nm). These results indicate the **CP1** and **CP2** exhibit stable PL color as temperature changes [48,49]. It can be clearly seen from the temperature-dependent fluorescence emission spectra that the **CP1** shows the reduced TQ effect at high temperature compared to **CP2** (Figs. 4a-d). With increasing temperature, the PL of **CP1** changes from orange at low temperature (80 K) to yellow at high temperature (500 K). The variation of the CIE coordinates is consistent with the PL emission shift as temperature changes. The corresponding CIE coordinates show slightly change from (0.52, 0.47) at 80 K to (0.48, 0.49) at 500 K (Fig. 4e). However, the luminescence color of **CP2** shows the negligible change with increasing temperature, with the corresponding CIE coordinates of (0.43, 0.54) at 80 K and (0.43, 0.52) at 400 K (Fig. 4f).

Thermogravimetric analysis (TGA) was used to investigate the thermal stability of the complexes **CP1** and **CP2**. From the TGA curve (Fig. S7 in Supporting information), two complexes show high thermal stability and evidence two-step decomposition. The first weight loss of about 39%–44% of all complexes was observed between 200 °C and 400 °C, due to the removal of halogens and partial ligand. A second weight loss between 400 °C and 650 °C can be ascribed to the complete removal of the remaining ligands.

Considering the enhanced PLQY and PL thermal stability, we fabricated the LEDs devices by incorporating **CP1** and **CP2** phos-

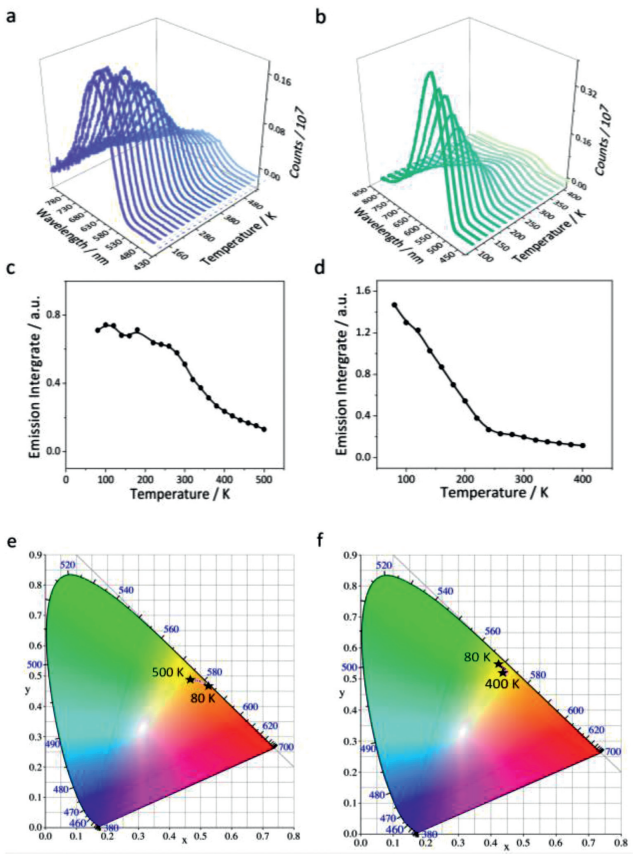

Fig. 4. The variable-temperature PL spectra of (a) **CP1** and (b) **CP2**. The temperature-dependent emission integrals of (c) **CP1** and (d) **CP2**. Variable-temperature CIE coordinates of (e) **CP1** and (f) **CP2**.

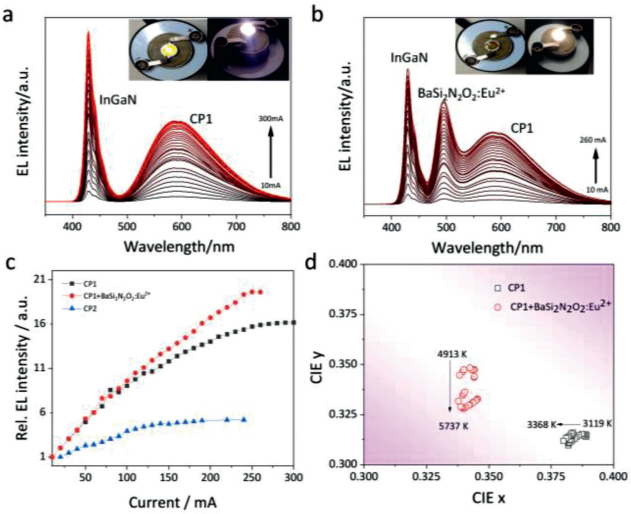

Fig. 5. (a) EL spectra of **CP1**-prototype LED with a 428-nm LED chip under flux operating currents of 10–300 mA. (b) EL spectra of integrated **CP1** and commercial $BaSi_2N_2O_2:Eu^{2+}$ pc-wLED with a blue LED chip (λ_{max} = 428 nm) under flux operating currents of 10–260 mA. The insets show the photographs of the device with power off (left) and power on (right). (c) Current-dependent EL intensity for single-component **CP1** and its dual-component wLED, as well as single-component **CP2**. (d) CIE chromaticity coordinates of **CP1**-prototype wLED (black square) as well as the commercial $BaSi_2N_2O_2:Eu^{2+}$-based pc-wLED (red circle).

phors, respectively, with a blue LED chip (λ_{max} = 428 nm) and investigated the LED performance. The results of single-component LEDs are shown in Fig. 5a and Fig. S8 (Supporting information). The electroluminescence (EL) intensities increase with increasing currents below 300 mA (Table S5 in Supporting information). For **CP1**-prototype pc-LED, the EL intensity obtains a 16-fold increase from 10 mA to 300 mA with slight CIE coordinates change between (0.389, 0.314) and (0.380, 0.312), which deviates from the CIE coordinates (0.33, 0.33) of ideal white light. The corresponding CCT values vary between 3119 K and 3368 K, demonstrating the warm white-light emission property [50]. In contrast, the single-component **CP2**-prototype LED device exhibits white light emission with CIE chromaticity coordinates close to (0.33, 0.33) (Fig. S9 and Table S6 in Supporting information), the CIE chromaticity coordinate moving of **CP2**-prototype LED in relative to the **CP1** counterpart is consistent with the steady-state PL emission spectra as shown in Fig. 3a. However, the EL intensities exhibit the significant reduction at high basis current, which is likely to be caused by the serious TQ effect. As a result, the **CP2**-prototype wLED device shows the low CRI value (*ca.* 77.5).

To demonstrate the potential of practical applications as ideal pc-wLEDs devices, we continued to fabricate the dual-component **CP1**-prototype pc-wLED through incorporating $BaSi_2N_2O_2:Eu^{2+}$ commercial phosphor as the blue-green component [51]. As a result, the EL spectra cover the whole visible region from 400 nm to 800 nm (*i.e.*, a white-light emission) and the EL intensities linearly increase as the current increases in the range of 10–260 mA (Figs. 5b and c). The PL color stability at the different currents was recorded. Compared to the single-component LED, the dual-component **CP1**-prototype pc-wLED shows the reduced quenching effect at high basis current (>100 mA). The CIE x (*ca.* 0.330) and CIE y (*ca.* 0.330) of **CP1**-prototype dual-component wLED remain basically unchanged, in the range (10–260 mA) of flux current (Fig. 5d and Table S7 in Supporting information), exhibiting excellent white-emissioin stability [52]. The average CRI value of **CP1**-prototype dual-component wLED is as high as 91.6 with a CCT of 5054 K in a flux current range of 10–260 mA. Hence, the ideal CCT and high CRI value show the excellent white-light properties of the **CP1**-prototype pc-wLED.

In summary, with suitably expanded π-conjugated system of benzotriazole derivatives, we have prepared two copper(I)-iodide coordination network materials as intense yellow-emitting phosphors with a blue-light excitation. The photophysical investigations indicate that the yellow phosphors emit an efficient room-temperature phosphorescence with excellent photostability. Owing to the enhanced efficiency and stability, the blue-light-excitable coordination network materials can be considered a promising phosphor for fabrication of high-quality white LEDs. These results demonstrate an idea example for preparing blue-light-excitable Cu(I) coordination networks as yellow phosphors which are necessary for high-performance white LED devices.

Declaration of competing interest

All of the authors have approved the manuscript submission, without conflicts of interest to declare.

Acknowledgments

We are thankful for financial support from the PAPD of Jiangsu Higher Education Institutions. This work is supported by the National Natural Science Foundation of China (No. 92161121).

Supplementary materials

Supplementary material associated with this article can be found, in the online version, at doi:10.1016/j.cclet.2023.108600.

References

[1] H.V.R. Dias, H.V.K. Diyabalanage, M.A. Rawashdeh-Omary, et al., J. Am. Chem. Soc. 125 (2003) 12072–12073.
[2] M. Chen, C. Ye, C. Dai, et al., Adv. Opt. Mater. 10 (2022) 2200278.
[3] D.M. Zink, D. Volz, T. Baumann, et al., Chem. Mater. 25 (2013) 4471–4486.
[4] S. Pimputkar, J.S. Speck, S.P. DenBaars, et al., Nat. Photon. 3 (2009) 180–182.
[5] W. Meng, C. Wang, Y. Li, et al., Chem. Eur. J. 29 (2023) e202202675.
[6] M. Li, Z. Cheng, X. Wang, et al., J. Phys. Chem. Lett. 12 (2021) 8237–8245.
[7] Y. Fang, W. Liu, S.J. Teat, et al., Adv. Funct. Mater. 27 (2017) 1603444.
[8] J. Huang, B. Su, E. Song, et al., Chem. Mater. 33 (2021) 4382–4389.
[9] H.H. Deng, Q.Q. Zhuang, K.Y. Huang, et al., Nanoscale 12 (2020) 15791–15799.
[10] Q. Dai, C.E. Duty, M.Z. Hu, Small 6 (2010) 1577–1588.
[11] W. Zhaxi, M. Li, J. Wu, et al., Molecules 27 (2022) 4441.
[12] Y. Xue, Y. Chen, G. Li, et al., Chin. Chem. Lett. 35 (2024) 108447.
[13] W. Mi, N. Shao, Chin. Chem. Lett. 33 (2022) 298–303.
[14] W. Liu, Y. Fang, J. Li, Adv. Funct. Mater. 28 (2018) 1705593.
[15] W. Liu, Y. Fang, G.Z. Wei, et al., J. Am. Chem. Soc. 137 (2015) 9400–9408.
[16] Z. Wang, B. Chen, A.S. Susha, et al., Adv. Sci. 3 (2016) 1600182.
[17] Z. Ma, Z. Shi, C. Qin, et al., ACS Nano 14 (2020) 4475–4486.
[18] K. Xu, B.L. Chen, R. Zhang, et al., Dalton Trans. 49 (2020) 5859–5868.
[19] G. Li, H. Ye, F. Zhu, et al., Chin. Chem. Lett. 30 (2019) 1931–1934.
[20] H. Miao, X. Pan, M. Li, et al., Inorg. Chem. 61 (2022) 18779–18788.
[21] R. Czerwieniec, J. Yu, H. Yersin, Inorg. Chem. 50 (2011) 8293–8301.
[22] Y. Liu, S.C. Yiu, C.L. Ho, et al., Coord. Chem. Rev. 375 (2018) 514–557.
[23] L.T. Wang, Z.Z. Ma, F. Zhang, et al., J. Mater. Chem. C 9 (2021) 6151–6159.
[24] J. Troyano, F. Zamora, S. Delgado, Chem. Soc. Rev. 50 (2021) 4606–4628.
[25] D.M. Zink, T. Baumann, J. Friedrichs, et al., Inorg. Chem. 52 (2013) 13509–13520.
[26] K. Tsuge, Y. Chishina, H. Hashiguchi, et al., Coord. Chem. Rev. 306 (2016) 636–651.
[27] M. Trose, F. Nahra, C.S.J. Cazin, Coord. Chem. Rev. 355 (2018) 380–403.
[28] Y.S. Liu, Y. Liu, X.W. Ma, et al., Chin. Chem. Lett. 25 (2014) 775–778.
[29] P.C. Ford, Coordin. Chem. Rev. 132 (1994) 129–140.
[30] S. Perruchas, X.F. Le Goff, S. Maron, et al., J. Am. Chem. Soc. 132 (2010) 10967–10969.
[31] H. Kitagawa, Y. Ozawa, K. Toriumi, Chem. Commun. 46 (2010) 6302–6304.
[32] P.C. Ford, E. Cariati, J. Bourassa, Chem. Rev. 99 (1999) 3625–3648.
[33] V. Arnd, K. Horst, J. Am. Chem. Soc. 108 (1986) 7211–7212.
[34] H. Miao, Y. Zhou, P. Wang, et al., Chem. Commun. 59 (2023) 1229–1232.
[35] T. Wu, S. Jiang, P.N. Samanta, et al., Chem. Commun. 56 (2020) 12057–12060.
[36] D.M. Zink, M. Bächle, T. Baumann, et al., Inorg. Chem. 52 (2013) 2292–2305.
[37] B. Huitorel, H. El Moll, R. Utrera-Melero, et al., Inorg. Chem. 57 (2018) 4328–4339.
[38] I.D. Strelnik, I.R. Dayanova, I.E. Kolesnikov, et al., Inorg. Chem. 58 (2019) 1048–1057.
[39] C.M. Che, Z. Mao, V.M. Miskowski, et al., Angew. Chem. Int. Ed. 39 (2000) 4084–4088.
[40] X.Y. Chang, K.H. Low, J.Y. Wang, et al., Angew. Chem. Int. Ed. 55 (2016) 10312–10316.
[41] Z. Liu, P.I. Djurovich, M.T. Whited, et al., Inorg. Chem. 51 (2012) 230–236.
[42] J.M. Poblet, M. Bénard, Chem. Commun. (1998) 1179–1180.
[43] D. Sun, S. Yuan, H. Wang, et al., Chem. Commun. 49 (2013) 6152.
[44] H.V.R. Dias, H.V.K. Diyabalanage, M.G. Eldabaja, et al., J. Am. Chem. Soc. 127 (2005) 7489–7501.
[45] L.X. Hu, M. Gao, T. Wen, et al., Inorg. Chem. 56 (2017) 6507–6511.
[46] S. Wang, E.E. Morgan, S. Panuganti, et al., Chem. Mater. 34 (2022) 3206–3216.
[47] Y. Wang, J. Wang, H.-X. Zhang, et al., Organometallics 37 (2018) 2491–2499.
[48] T. Wen, D.X. Zhang, J. Liu, et al., Chem. Commun. 49 (2013) 5660–5662.
[49] T. Wen, D.X. Zhang, H.X. Zhang, et al., Chem. Commun. 50 (2014) 8754–8756.
[50] X. Ma, X. Xu, F. Duan, et al., Adv. Opt. Mater. (2021) 2101461.
[51] S. Huang, E. Wang, J. Tong, et al., Chin. Chem. Lett. 34 (2023) 108008.
[52] G.L. Yang, H.Z. Zhong, Chin. Chem. Lett. 27 (2016) 1124–1130.